

Particle-Based COVID-19 Simulator with Contact Tracing and Testing

Askat Kuzdeuov, *Member, IEEE* Aknur Karabay, Daulet Baimukashev, Bauyrzhan Ibragimov, and Huseyin Atakan Varol*, *Senior Member, IEEE*

Abstract—Goal: COVID-19 pandemic has emerged as the most severe public health crisis in over a century. As of December 2020, there are more than 60 million cases and 1.4 million deaths. For informed decision making, reliable statistical data and capable simulation tools are needed. Our goal is to develop an epidemic simulator which can model the effects of random population testing and contact tracing. **Methods:** Our simulator models each individuals as particles with position, velocity and epidemic status states on a 2D map and runs a SEIR epidemic model with contact tracing and testing modules. The simulator is available in GitHub under MIT license. **Results:** The results show that the synergistic use of contact tracing and massive testing is effective in suppressing the epidemic (the number of deaths was reduced by 72%). **Conclusions:** Particle-based COVID-19 simulator enables the modeling of intervention measures, random testing and contact tracing, for epidemic mitigation and suppression.

Index Terms—Epidemic simulator, COVID-19, particle-based simulation, SEIR model, epidemic control, contact tracing, random testing.

Impact Statement- Our particle-based epidemic simulator calibrated with COVID-19 data models each individual as a unique particle with location, velocity and epidemic state, enabling consideration of contact tracing and testing measures.

I. INTRODUCTION

THE COVID-19 has emerged as the most threatening health care crisis in over a century, spreading rapidly throughout the world. The first cases were identified in Wuhan, China (December 2019), and within months the World Health Organization declared the disease as a pandemic (11 March 2020) [1]. The propagation of the virus has increased rapidly in spite of unprecedented government interventions intended to suppress and mitigate the spread; as of 29 November 2020, more than 61.6 million cases with 1.44 million deaths have been reported [2]. However, the actual number of cases is likely significantly higher due to limited testing and the high percentage of asymptomatic cases [3].

Propagation was accelerated by the multiple convergent factors, led first by the fact that it is a novel coronavirus to

A. Kuzdeuov, A. Karabay, D. Baimukashev, B. Ibragimov, and H.A. Varol are with the Institute of Smart Systems and Artificial Intelligence (ISSAI), Nazarbayev University, 010000, Nur-Sultan, Republic of Kazakhstan. Email addresses: {askat.kuzdeuov, aknur.karabay, daulet.baimukashev, bauyrzhan.ibragimov, ahvarol}@nu.edu.kz

Corresponding author: Huseyin Atakan Varol

which there is no existing resistance amongst the population, nor an effective vaccine. Different vaccines against COVID-19 have been developing at a historic rate, but their effectiveness and safety are still open question [4]. Until such time as a vaccine emerges, and can be distributed at scale, the only recourse to retard the spread of the disease is what are known as non-pharmaceutical interventions (NPIs) such as quarantines, travel restrictions [5], online education [6], and large-scale virus testing with comprehensive contact tracing of infected individuals [7], [8].

The lockdown policies slow down the propagation of the disease but they also inflict substantial social and economic damage [9], [10], and when done indiscriminately the negative effects are non-trivial; interdiction measures should be enacted in ways that mitigate disease spread while minimizing negative effects. One way to achieve a more nuanced approach, with less collateral damage, is the use of computer models and simulations.

One of the earliest epidemic models, Susceptible-Infected-Recovered (SIR) [11], divides the population into three compartments. In the first compartment, susceptible (S), individuals are vulnerable but not infected. In the second compartment, infected (I), individuals are infected and capable to transmit the disease to the susceptible individuals. The last compartment, recovered (R), contains individuals who have overcome the disease. The recovered individuals are assumed to have acquired some level of immunity to the disease, thus they have a lower probability of reinfection compared to susceptible individuals.

The compartmental models were widely used in modeling the spread of the COVID-19 [12]–[14]. Despite their popularity, the compartmental models have several limitations due to the simplifying assumptions that do not represent actual viral propagation. For instance, compartmental models do not consider each individual separately. Therefore, the mobility and current epidemic state of each individual, the moments of getting infected and recovered are omitted. As a result, the contact tracing and testing policies at the individual level cannot be implemented.

A number of works on epidemic simulation at the individual level can be found in the literature. For instance, a particle-modeling approach based on the Monte Carlo algorithm was developed to simulate the spread of the COVID-19 [15]. The results show that periodic lockdown and strict social distancing might help to keep the infection rate under control. A stochastic agent-based model was employed for simulating the COVID-19 in France [16]. An SEIR agent-based model was imple-

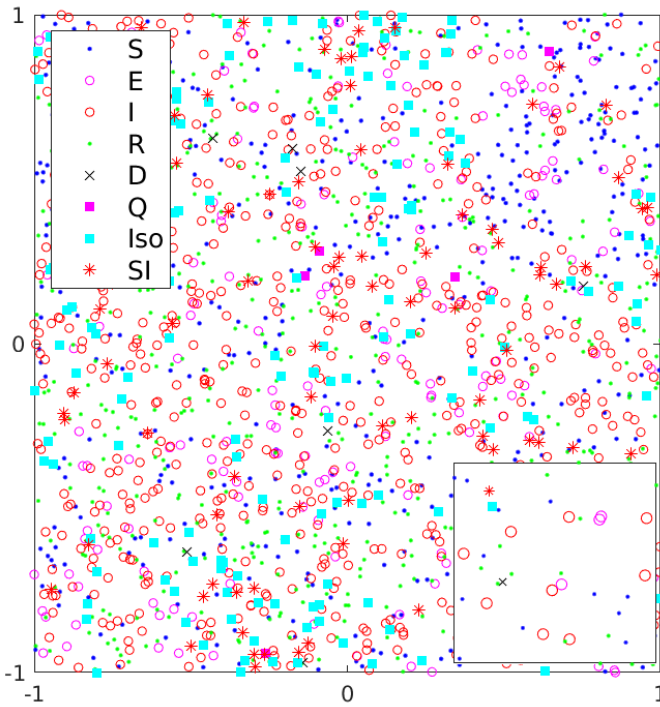


Fig. 1. Visualization of the particles on the map including their epidemic states.

mented to analyze different social distancing interventions in [17]. An agent-based simulation was implemented by Bicher et al. [18] to estimate the effectiveness of contact tracing policies.

In this work, we have developed a particle-based simulator which models each individual as a unique particle with a location, velocity and epidemic state (see Fig. 1). To the best of our knowledge, it is the first particle-based SEIR model, with contact tracing and testing modules, that was calibrated with actual COVID-19 data. The particles randomly move on a square 2D map, and become infected if they enter proximity of an infectious particle closer than a predefined physical distance. The contact tracing module is based on the use of a mobile app and it stores the list of contacts for each particle such that if the particle is determined to be infected then all particles in the list are quarantined or isolated. The testing module simulates the massive random testing of the population. The module considers test sensitivity and specificity [19]. This way, the simulator is able to simulate different scenarios and mitigation policies.

The rest of the paper is organized as follows: In Section II, we introduce our method of implementing the particle simulator. In Section III, we calibrate the particle simulator using real COVID-19 data. Afterward, we simulate the model using different contact tracing ratios and daily number of tests per thousand people. In Section IV, we discuss the simulation results, and the Section V concludes our work.

II. MATERIALS AND METHODS

A. Particle Model

In this work, each individual is considered as a particle p and modeled as

$$p = [x, v, e, t, a, ts] \quad (1)$$

where $x \in \mathbb{R}^2$ is the position of a particle on the map (see Fig. 1), $v \in \mathbb{R}^2$ is the particle velocity, e is the epidemic state of the particle (i.e. susceptible, exposed, infected, recovered, dead, quarantined, isolated, or severe infected), t is the time of the particle in the current epidemic state and it is incremented by the sampling time Δt at each iteration of the simulation, a denotes the availability of the contact tracing application, ts is COVID-19 test result of the particle.

The current position and velocity of n particles are stored in matrices $X \in \mathbb{R}^{n \times 2}$ and $V \in \mathbb{R}^{n \times 2}$, and constrained by $-1 \leq x_{ij} \leq 1$, $-v_{max} \leq v_{ij} \leq v_{max}$ for all particles $i = 1, \dots, n$ and two dimensions $j = 1, 2$. The initial values are set randomly by taking into account the imposed constraints. The velocity matrix $V \in \mathbb{R}^{n \times 2}$ is updated at each iteration κ ($1 \leq \kappa \leq T/\Delta t$) in the simulation as

$$V_{\kappa} = V_{\kappa-1} + \lambda(R_{\kappa} - 0.5) \quad (2)$$

where $R_{\kappa} \in \mathbb{R}^{n \times 2}$ is a matrix of uniformly distributed random numbers in the interval $[0, 1]$, and λ is a momentum that allows to control velocity change. Velocities are reset to zero if they exceed the maximum allowed speed v_{max} . In addition, dead, quarantined, isolated, and severe infected (hospitalized) particles are considered not moving, i.e. their velocities are also set to zero.

Then, the position matrix $X \in \mathbb{R}^{n \times 2}$ is updated as

$$X_{\kappa} = X_{\kappa-1} + V_{\kappa} \Delta t$$

$$x_{ij} = \begin{cases} x_{ij}, & \text{if } \|x_{ij}\| \leq 1 \\ -x_{ij}, & \text{otherwise} \end{cases} \quad (3)$$

such that if particles reach one of the borders of the map they appear on the opposite side. This is necessary to keep all particles always inside the map.

B. Particle-Based SEIR Simulator

The particle-based simulator consists of four superstates: Susceptible (S^s), Exposed (E^s), Infected (I^s), and Recovered (R^s). Transitions between states are shown in Fig. 2. The Exposed superstate (E^s) is composed of Exposed (E) and Quarantined (Q) states. The Quarantined (Q) state consists of True Quarantined (TQ) and False Quarantined (FQ) substates. Similarly, the Infected superstate (I^s) consists of Infected (I), Isolated (Iso), and Severe Infected (SI) states. The Isolated (Iso) state also contains two substates: True Isolated ($TIso$) and False Isolated ($FIso$). To avoid confusions between the superstates (e.g. E^s) and states (e.g. E), we will refer to only states further. Also, when particles transition from the current superstate to another, their time t in the current superstate is reset to zero and starts over in the new superstate. The time is not changed if transitions occur between states of the same superstate.

Quarantined state go back to the Susceptible state.

III. RESULTS

A. Particle-Based SEIR Simulation of Lecco

In this section, we simulate the epidemic in the Lecco province of Italy. Lecco is located in the Lombardy region which was the epicenter of the COVID-19 outbreak in Italy. We chose this province because the epidemic timeline of Lombardy is well-established, and official statistics of daily epidemic data for the region and its provinces has been shared with public since 24 February 2020 [20]. The total number of particles n was set to 337,000 (i.e. population of Lecco). The other parameters of the simulation are shown in Table II. In order to tune parameters of the model, we relied on the officially reported number of deaths and total cases. However, according to the seroprevalence survey results presented on 3 August 2020 by the Italian Ministry of Health [21], it was estimated that 1,482,000 people have encountered the virus in Italy which is six times larger than the officially registered cases. Therefore, we assume that the actual number of total cases in Lecco also six times larger than the registered cases. Because the daily deaths for provinces are not available in [20], we used proportional amount from total deaths officially published for Lombardy region.

We started the simulation on 1 January 2020, based on the results in [22], with initially 10 exposed particles. The length of the simulation was 200 days. Regarding the parameters of the testing module, there was no official data on used test kits and amount of daily tests per thousand people for Lecco. Therefore, we estimated the daily tests per thousand people θ as 0.5 for the considered period in the simulation based on the testing data for whole Italy [23]. For the test sensitivity sn and specificity sp , we used values of most commonly manufactured tests kits [24]. In order to imitate the lock-down in Lecco, we decreased the maximum speed of particles v_{max} and λ according to the timeline of events, and when the lock-down was lifted on 3 June 2020, we returned them to their initial values assuming that people started traveling as usual. However, the contact threshold x_{thr} was decreased slightly assuming that the population started wearing masks and keeping physical distancing.

The averaged results of ten simulations are shown in Fig. 3 with the standard deviations for the total cases and deaths. According to the reported data for the province of Lecco [20], new daily cases increased significantly starting from the middle of March and remained high until the middle of April. Thus, we conclude that our simulator predicted the peak of the epidemic correctly. Also, the average number of total cases was estimated

approximately more than five times higher than the reported numbers which is similar to the results of the seroprevalence test for the whole Italy.

B. Simulations with Contact Tracing and Testing Modules

In this section, we analyze the impact of randomly testing the population and tracing contacts of positive tested individuals in reducing the spread of the epidemic. First, we considered the case of massively testing the population without contact tracing policy. Thus, we set β to zero and conducted simulations for different values of $\theta = \{0, 5, 10, 15, 20\}$. The results of the simulations are shown in the top row of Fig. 4. According to the results in the Fig. 4a and Fig. 4b, the number of particles in the Isolated and Quarantined states increases with the increased value of θ . Consequently, the number of infected particles, at the peak of the epidemic, reduced gradually from 4,925 ($\theta = 0$) to 3,633 ($\theta = 5$), 2,926 ($\theta = 10$), 2,428 ($\theta = 15$), and to 1,841 ($\theta = 20$) (see Fig. 4c).

Similarly, we examined the effect of the contact tracing policy without randomized testing of the population. We set θ to zero and simulated with different values of $\beta = \{0.0, 0.25, 0.5, 0.75, 1.0\}$. In this case, we traced particles that were in contact only with the severe infected particles (i.e. hospitalized) because infected and exposed particles can be found with randomly testing the population. The results of the simulations are shown in the bottom row of the Fig. 4. According to the Fig. 4d and Fig. 4e, the number of particles in the Isolated and Quarantined states increased with the increased value of β . As a result, the number of infected particles at the peak of the epidemic, decreased from 4,925 ($\beta = 0$) to 4,487 ($\beta = 0.25$), 4,019 ($\beta = 0.5$), 3,030 ($\beta = 0.75$), and to 2,273 ($\beta = 1.0$) (see Fig. 4f).

Next, we considered utilization of concurrent contact tracing and massive testing. The considered numbers of daily tests per thousand people and the contact tracing ratios were $\theta = \{0, 10, 20\}$ and $\beta = \{0, 0.5, 1.0\}$, respectively. According to the results in Figs. 5a and 5b, for $\theta = 10$ the enabled contact tracing module increases the number of isolated and quarantined particles. However, for $\theta = 20$ the numbers decrease with the increased contact tracing ratios. The reason is that the higher number of tests allow to find infected and exposed particles at the beginning of the epidemic faster, and additional contact tracing makes this process even faster. Therefore, at the peak of the epidemic we get a lower number infected and exposed particles, and as a result less number of isolated and quarantined particles. Nevertheless, in both cases the contact tracing module decreased the number of infected and exposed particles further as shown in Fig. 5c and Fig. 5d. The number of infected particles, at the peak of the epidemic, dropped from 2,926 ($\theta = 10, \beta = 0$) to 2,360 ($\theta = 10, \beta = 0.5$) and 2,071 ($\theta = 10, \beta = 1.0$). The effect became more pronounced with increased daily testing. Specifically, the number of infected particles reduced from 1,841 ($\theta = 20, \beta = 0$) to 1,547 ($\theta = 20, \beta = 0.5$) and to 1,004 ($\theta = 20, \beta = 1.0$).

IV. DISCUSSION

The simulation results showed that the random testing is more efficient compared to the contact tracing module in

TABLE II. Simulation Parameters for Lecco.

v_{max} (Days)	λ (Days)	x_{thr} (Days)	ϵ_{exp}	ϵ_{qua}	ϵ_{sev}	t_{exp}
0.02 (0-55)	0.002 (0-55)					
0.012 [55-71]	0.0012 [55-71]	8.6e-5 (0-154)				
0.006 [71-82]	0.0006 [71-82]	6.9e-5 [154-200]	0.7	0.3	0.3	5
0.004 [82-154]	0.0004 [82-154]					
0.02 [154-200]	0.002 [154-200]					
t_{inf}	sir	γ_{mor}	β	θ	sn	sp
14	0.02	0.15	0	0.5	0.95	0.99

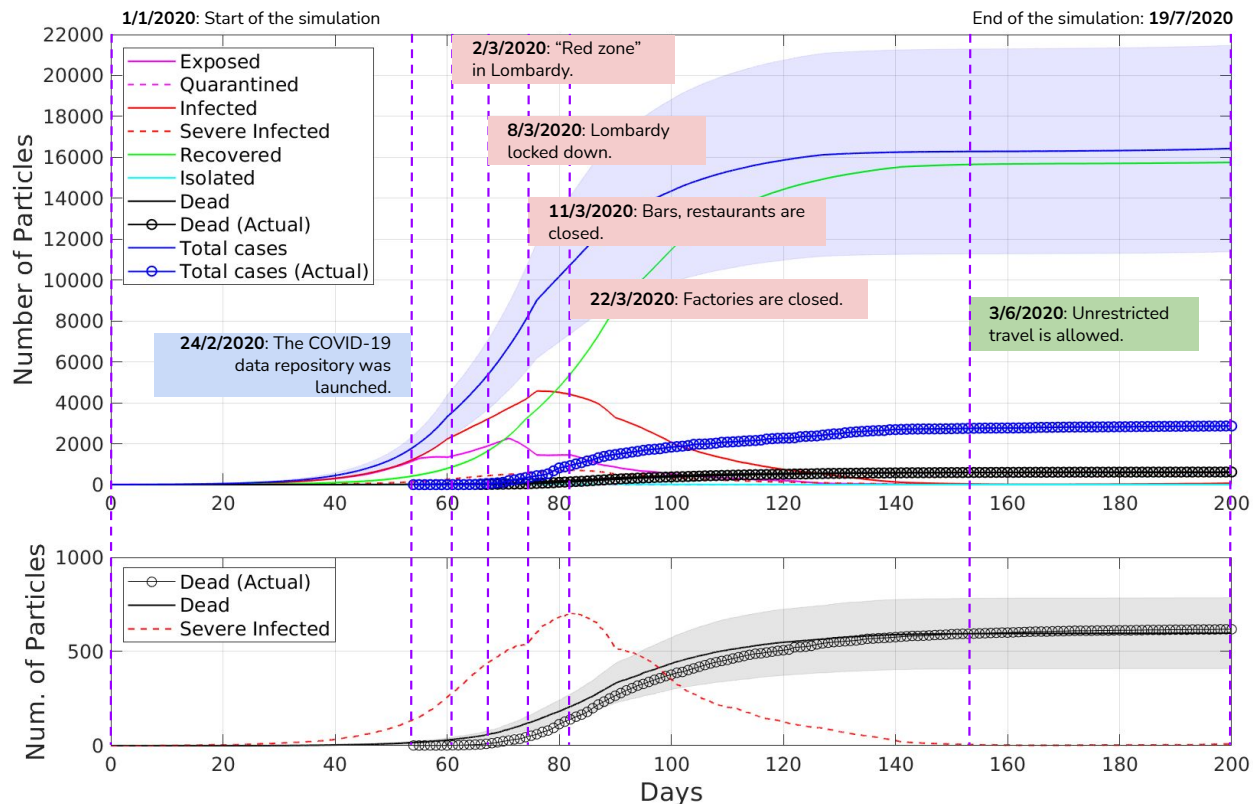


Fig. 3. The averaged results of ten simulations for the province of Lecco. Upper plot shows the states of the epidemic simulation versus time and the dates of important NPIs. One standard deviation around the average Total case curve is shaded. Bottom plot shows the number of Severe Infected particles, the number of deaths in the simulation, and the actual number of deaths attributed to COVID-19. One standard deviation around the average Dead state curve is shaded.

reducing the number of infected particles when they are used separately. When we use the contact tracing without random testing, we trace contacts of severe infected particles. The exposed and infected particles continue infecting susceptible particles until they transition to the Severe Infected state. Therefore, the contact tracing module is not effective alone. Also, if we look at the zoomed subplots in Fig. 4c and Fig. 4f, we see that both methods does not preserve from the second wave of the epidemic after the lifting of restrictions on 3 June 2020.

On the other hand, synergistic use of two modules showed the most effective results. Namely, the massive testing strategies with $\theta = 10$, $\beta = 0$ and $\theta = 20$, $\beta = 0$ reduced the total number of deaths from 630 ($\theta = 0$, $\beta = 0$) to 440 (30%) and 294 (53%). Then, in simulations with 50% ($\beta = 0.5$) of the population using the contact tracing app, massive testing $\theta = 10$ and $\theta = 20$ reduced the total number of deaths up to 40% (374 deaths) and 60% (249), respectively. The reduction in the number of deaths reached its maximum with the ubiquitous contact tracing ($\beta = 1.0$). The simulations returns 323 (48% reduction) and 177 (72% reduction) for ($\theta = 10$, $\beta = 1.0$) and ($\theta = 20$, $\beta = 1.0$), respectively. Also, if we look at zoomed subplots in Fig. 5c, d, and e, we see that synergistic use of two modules allows to prevent the emergence of the second wave of the epidemic. These results reveal the importance of immediate isolation of contacts of positive tested particles in

preventing the spread of the epidemic.

Even though the modeling of individuals as particles enables the implementation of contact tracing and massive testing, our simulator has several limitations. Firstly, our map is a unit square with the individuals distributed randomly and moving freely without obstacles. In real world, there are obstacles, e.g. buildings and geographic objects such as rivers and mountains. Also, the population density differs substantially in different regions of a city or province. The probability of infection is also lower in open spaces than in confined ones. Secondly, the mortality rate for COVID-19 is age and gender dependent [25]. Our particles are identical, i.e. demographics properties such as age and gender are not considered. Presumably, the simulator can be enriched by adding the demographics profiles and related risk probabilities for more realistic transitions from the Severe Infected to Dead state. However, this would increase the number of simulation parameters significantly and make the model calibration harder. Thirdly, the simulator also does not consider the interaction networks of individuals. However, in reality, individuals have a number of contacts with whom they interact regularly, e.g. family members, colleagues, and close friends.

V. CONCLUSION

We developed a particle-based SEIR simulator with contact tracing and testing regimens. The main advantage of our

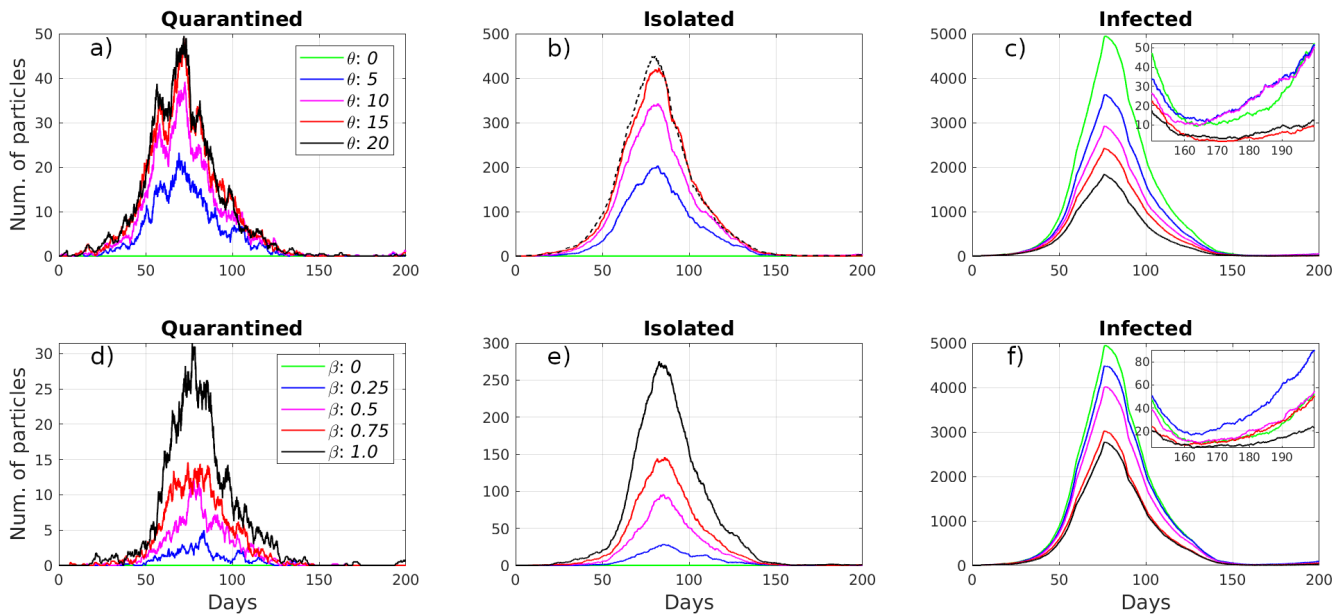


Fig. 4. Simulation results of using only the random testing module: a, b, c, and using only the contact tracing module: d, e, f.

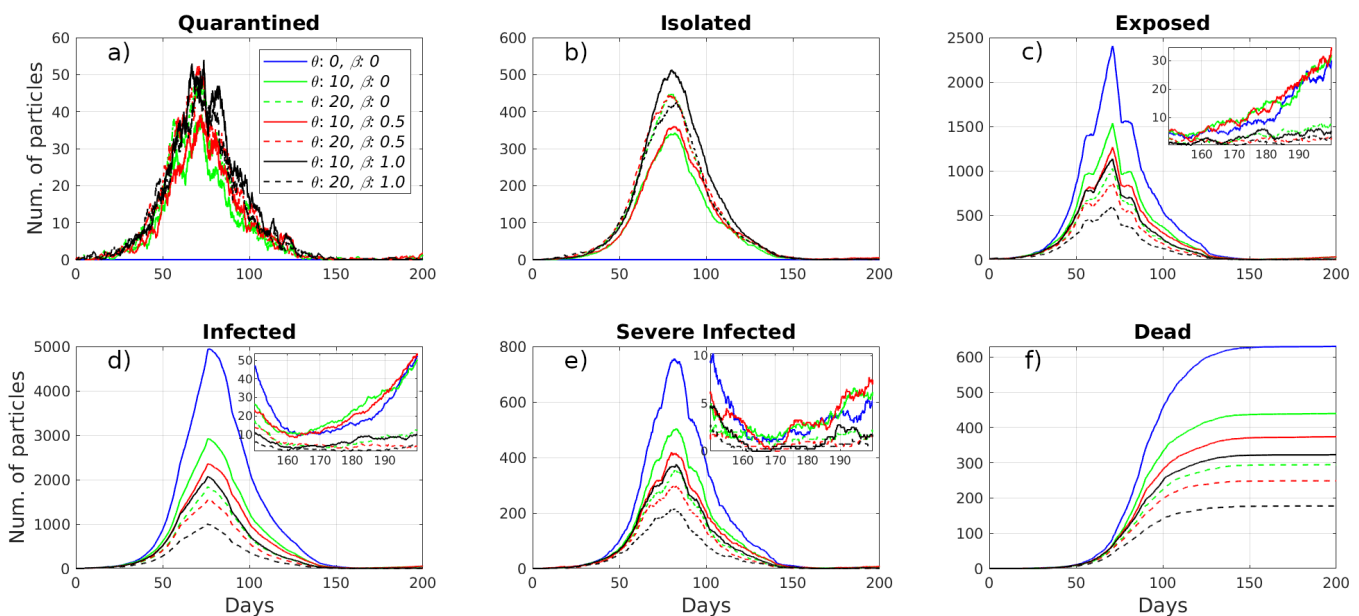


Fig. 5. Simulation results for the different combinations of random testing and contact tracing modules.

simulator as compared to the compartmental SEIR model is that it models each individual as a particle, thus enabling more realistic simulation of disease propagation and the impact of intervention strategies for suppression and mitigation. We demonstrated that the simulator can model a real epidemic in accordance with the actual timeline of events and deployment of intervention strategies. We also investigated the impact of contact tracing and testing strategies on the propagation of the disease; results showed that the most effective approach is an aligned strategy of testing and contact tracing. In future works, the particle-based simulator can be used to simulate the

spread of the disease in more confined settings, such as inside of buildings (airports, schools, malls, and etc.) by modeling the moving particles according to the specific building layouts.

SUPPLEMENTARY MATERIALS

We implemented the simulator in MATLAB R2020. The source code was uploaded to GitHub¹ under MIT license. Also, we provide a video² that illustrates a random motion of a single particle, and also the visualization of particles motion on the 2D map with corresponding epidemic state transitions

¹<https://github.com/IS2AI/Particle-Based-COVID19-Simulator>

²<https://www.youtube.com/watch?v=BJfjmWfi6acfeature=youtu.be>

for three different scenarios. The first scenario for $\theta = 0$, $\beta = 0$ shows that the epidemic was suppressed in Lecco only due to the complete lock-down. The second scenario for $\theta = 20$, $\beta = 0$ illustrates that the lock-down with the additional random testing strategy can reduce the number of infected particles. However, in the previous two scenarios, the second wave of the epidemic starts after lifting lockdown. The third scenario with $\theta = 20$, $\beta = 1$ shows the effectiveness of the additional contact tracing strategy. This strategy significantly reduces the number of infected particles and also allows to prevent the second wave of the epidemic.

REFERENCES

- [1] WHO. (2020) Timeline of WHO's response to COVID-19. Last accessed on 2020-10-2: <https://www.who.int/news-room/detail/29-06-2020-covidtimeline>.
- [2] WHO. (2020) Coronavirus disease (COVID-19) outbreak situation. Last accessed on 2020-10-2: <https://www.who.int/emergencies/diseases/novel-coronavirus-2019>.
- [3] D. Oran and E. Topol, "Prevalence of asymptomatic SARS-CoV-2 infection," *Annals of Internal Medicine*, vol. 173, no. 5, pp. 362–367, 2020, pMID: 32491919. [Online]. Available: <https://doi.org/10.7326/M20-3012>
- [4] S. P. Kaur and V. Gupta, "COVID-19 Vaccine: A comprehensive status report," *Virus Research*, vol. 288, pp. 198 114–198 114, Oct 2020. [Online]. Available: <https://doi.org/10.1016/j.virusres.2020.198114>
- [5] M. U. G. Kraemer, C.-H. Yang, B. Gutierrez, C.-H. Wu, B. Klein, D. M. Pigott *et al.*, "The effect of human mobility and control measures on the COVID-19 epidemic in China," *Science*, vol. 368, no. 6490, pp. 493–497, 2020. [Online]. Available: <https://science.sciencemag.org/content/368/6490/493>
- [6] R. M. Viner, S. J. Russell, H. Croker, J. Packer, J. Ward, C. Stansfield *et al.*, "School closure and management practices during coronavirus outbreaks including COVID-19: A rapid systematic review," *The Lancet Child & Adolescent Health*, vol. 4, no. 5, pp. 397 – 404, 2020. [Online]. Available: <http://www.sciencedirect.com/science/article/pii/S235246422030095X>
- [7] D. Lee and J. Lee, "Testing on the move: South Korea's rapid response to the COVID-19 pandemic," *Transportation Research Interdisciplinary Perspectives*, vol. 5, p. 100111, 2020. [Online]. Available: <http://www.sciencedirect.com/science/article/pii/S2590198220300221>
- [8] V. J. Lee, C. J. Chiew, and W. X. Khong, "Interrupting transmission of COVID-19: Lessons from containment efforts in Singapore," *Journal of Travel Medicine*, vol. 27, no. 3, 03 2020, taaa039. [Online]. Available: <https://doi.org/10.1093/jtm/taaa039>
- [9] G. Bonaccorsi, F. Pierri, M. Cinelli, A. Flori, A. Galeazzi, F. Porcelli *et al.*, "Economic and social consequences of human mobility restrictions under COVID-19," *Proceedings of the National Academy of Sciences*, vol. 117, no. 27, pp. 15 530–15 535, 2020. [Online]. Available: <https://www.pnas.org/content/117/27/15530>
- [10] M. Nicola, Z. Alsafi, C. Sohrabi, A. Kerwan, A. Al-Jabir, C. Iosifidis *et al.*, "The Socio-Economic Implications of the Coronavirus and COVID-19 Pandemic: A Review," *International journal of surgery (London, England)*, pp. S1743–9191(20)30 316–2, Apr 2020. [Online]. Available: <https://doi.org/10.1016/j.ijssu.2020.04.018>
- [11] W. O. Kermack and A. G. McKendrick, "A contribution to the mathematical theory of epidemics," *Proc. of the Royal Society of London. Series A*, vol. 115, no. 772, pp. 700–721, 1927. [Online]. Available: <http://www.jstor.org/stable/94815>
- [12] A. Kuzdeuov, D. Baimukashev, A. Karabay, B. Ibragimov, A. Mirzakhmetov, M. Nurpeissov, M. Lewis, and H. Atakan Varol, "A network-based stochastic epidemic simulator: Controlling COVID-19 with region-specific policies," *IEEE Journal of Biomedical and Health Informatics*, vol. 24, no. 10, pp. 2743–2754, 2020.
- [13] Z. Yang, Z. Zeng, K. Wang, S.-S. Wong, W. Liang, M. Zanin *et al.*, "Modified SEIR and AI prediction of the epidemics trend of COVID-19 in China under public health interventions," *Journal of Thoracic Disease*, vol. 12, no. 3, pp. 165–174, Mar 2020. [Online]. Available: <https://pubmed.ncbi.nlm.nih.gov/32274081>
- [14] S. Sanche, Y. T. Lin, C. Xu, E. Romero-Severson, N. Hengartner, and R. Ke, "High contagiousness and rapid spread of severe acute respiratory syndrome coronavirus 2," *Emerging Infectious Disease Journal*, vol. 26, no. 7, p. 1470, 2020. [Online]. Available: <https://doi.org/10.3201/eid2607.200282>
- [15] H. De-Leon and F. Pederiva, "Particle modeling of the spreading of coronavirus disease (COVID-19)," *Physics of Fluids*, vol. 32, no. 8, p. 087113, 2020. [Online]. Available: <https://doi.org/10.1063/5.0020565>
- [16] N. Hoertel, M. Blachier, C. Blanco, M. Olifson, M. Massetti *et al.*, "A stochastic agent-based model of the SARS-CoV-2 epidemic in France," *Nature Medicine*, vol. 26, no. 9, pp. 1417–1421, Sep 2020. [Online]. Available: <https://doi.org/10.1038/s41591-020-1001-6>
- [17] P. C. L. Silva, P. V. C. Batista, H. S. Lima, M. A. Alves, F. G. Guimarães, and R. C. P. Silva, "COVID-ABS: An agent-based model of COVID-19 epidemic to simulate health and economic effects of social distancing interventions," *Chaos, Solitons, and Fractals*, vol. 139, pp. 110 088–110 088, Oct 2020. [Online]. Available: <https://doi.org/10.1016/j.chaos.2020.110088>
- [18] M. R. Bicher, C. Rippinger, C. Urach, D. Brunmeir, U. Siebert, and N. Popper, "Agent-based simulation for evaluation of contact-tracing policies against the spread of SARS-CoV-2," *medRxiv*, 2020. [Online]. Available: <https://www.medrxiv.org/content/early/2020/09/17/2020.05.12.20098970>
- [19] R. Trevethan, "Sensitivity, specificity, and predictive values: Foundations, pliability, and pitfalls in research and practice," *Frontiers in Public Health*, vol. 5, p. 307, 2017. [Online]. Available: <https://www.frontiersin.org/article/10.3389/fpubh.2017.00307>
- [20] P. del Consiglio dei Ministri Dipartimento della Protezione Civile. (2020) Dati COVID-19 Italia. Last accessed on 2020-10-2: <https://github.com/pcm-dpc/COVID-19>.
- [21] M. della Salute. (2020) Primi risultati dell'indagine di sieroprevalenza SARS-CoV-2. Last accessed on 2020-10-2: http://www.salute.gov.it/imgs/C_17_notizie_4998_0_file.pdf.
- [22] D. Cereda, M. Tirani, F. Rovida, V. Demicheli, M. Ajelli, P. Poletti *et al.*, "The early phase of the COVID-19 outbreak in Lombardy, Italy," 2020.
- [23] O. W. in Data. (2020) Coronavirus COVID-19 Testing. Last accessed on 2020-10-2: <https://ourworldindata.org/coronavirus-testing>.
- [24] T. J. H. C. for Health Security. (2020) Serology-based tests for COVID-19. Last accessed on 2020-10-2: <https://www.centerforhealthsecurity.org/resources/COVID-19/serology/Serology-based-tests-for-COVID-19.html>.
- [25] C. Bonanad, S. García-Blas, F. Tarazona-Santabalbina, J. Sanchis, V. Bertomeu-González, L. Fácila *et al.*, "The Effect of Age on Mortality in Patients With COVID-19: A Meta-Analysis With 611,583 Subjects," *Journal of the American Medical Directors Association*, vol. 21, no. 7, pp. 915 – 918, 2020. [Online]. Available: <http://www.sciencedirect.com/science/article/pii/S1525861020304412>